Journal of Engineering
journal homepage: www.joe.uobaghdad.edu.iq
Number 7 Volume 26 July 2020

Mechanical and Energy Engineering

An Analytical Solution for the Maximum Tensile Stress and Stress Concentration Factor Investigations for Standard, Asymmetric fillets, Asymmetric Pressure Angle and Profile Shifted Helical and Spur Gears

Ahmed A. Toman *
M.Sc. Student
Engineering College-
University of Baghdad
E-mail: enginerahmed3@gmail.com

Mohammad Q. Abdullah
Prof. Dr.
Engineering College-
University of Baghdad
E-mail: mohq1969@yahoo.com

ABSTRACT

This research introduces a developed analytical method to determine the nominal and maximum tensile stress and investigate the stress concentration factor. The required tooth fillets parametric equations and gears dimensions have been reformulated to take into account the asymmetric fillets radiuses, asymmetric pressure angle, and profile shifting non-standard modifications. An analytical technique has been developed for the determination of tooth weakest section location for standard, asymmetric fillet radiuses, asymmetric pressure angle and profile shifted involute helical and spur gears. Moreover, an analytical equation to evaluate gear tooth-loading angle at any radial distance on the involute profile of spur and helical gears, (taking into account the effect of profile shift factor) has been derived. In addition, numerical solution for the evaluation of the maximum fillet tensile stress and the combined tensile stress concentration factor for the verification of the analytical method using computer-aided engineering software (ANSYS Version 18.1). The analytical and FE result have been compared and found to be very close. The most effective method for reducing the stress concentration factor have been found by applying negative profile shifting on asymmetric tooth with lower unloaded pressure angle and high loaded pressure angle and fillet radius, which can lead to an enhancement percentage of **(20%)** when using a ($35^o/20^o$) asymmetric spur gear of a (24) teeth number with a shift factor of ($-0.3m_o$) compared with standard (20^o) one.

Keywords: stress concentration factor, maximum tensile stress, helical gears, asymmetric teeth, profile shifted.

*Corresponding author Peer review under the responsibility of University of Baghdad.
https://doi.org/10.31026/j.eng.2020.07.15

Article received: 6/7/2019
Article accepted: 24/9/2019
Article published:1/7/2020

حل تحليلي رياضي لأقصى إجهاد شد والتحقيقات الخاصة بمعامل تركيز الإجهاد للتروس الحلزونية والعدلة ذات الاسنان القياسية، ذات شرائح جذر سن غير متناظرة، ذات زاويا ضغط غير متناظرة وذات ملف جانبيات مصحح.

أ.د. محمد قاسم عبد الله
قسم الهندسة الميكانيكية
جامعة بغداد- كلية الهندسة

أحمد علي تومان
قسم الهندسة الميكانيكية
جامعة بغداد- كلية الهندسة

الخلاصة

يقدم هذا البحث طريقة تحليلية مطورة لإيجاد إجهاد الشد الاسمي والاقصى وتحديد معامل تركيز الإجهاد وفحصه. تمت إعادة صياغة المعادلات البارامترية الخاصة بشرائح الأسنان المصممة وأبعاد التروس لتأخذ في نظر الاعتبار انصاف اقطار شرائح السن غير المتماثلة، زاويا الضغط غير المتماثلة وتصحيحات الجانبية غير القياسية. تم تطوير تقنية تحليلية مطورة من أجل تحديد أضعف قسم للأسنان ذات انصاف اقطار شرائح بكرية الشكل وغير متناظرة وزاوية ضغط غير متناظرة وتصحيح جانبيات للتروس الحلزونية والعدلة. علاوة على ذلك، تم اشتقاق معادلة تحليلية لإيجاد زاوية تحميل الأسنان عند أي مسافة نصف قطرية على المقطع الجانبي من المسننات والتروس الحلزونية والعدلة (مع مراعاة تأثير عامل تصحيح الجانبيات). بالإضافة إلى ذلك، تم أجراء الحل العددي لإيجاد قيم أقصى إجهاد الشد ومعامل تركيز الإجهاد للتحقق من الطريقة التحليلية باستخدام برنامج التحليل بمساعدة الكمبيوتر بطريقة العناصر المحددة (ANSYS الإصدار 18.1). تمت مقارنة النتيجة التحليلية والعددية ووجدت نتائج المقارنة بأنها قريبة جدًا. تم العثور على الطريقة الأكثر فاعلية لتقليل معامل تركيز الإجهاد باستخدام الأسنان غير المتماثلة ذات زاوية الضغط غسر محملة منخفضة وزاوية ضغط ذات قيم عالية للجانب المحمل مع معامل نصف قطر شرائح جذر السن عالية القيمة للجانب المحمل من السن.

الكلمات الرئيسية: معامل تركيز الإجهاد، أقصى إجهاد الشد، التروس الحلزونية، زوايا الضغط غير المتماثلة، تصحيحات جانبيات ملف الاسنان، شرائح جذر أسنان غير المتماثلة.

1. INTRODUCTION

Gears are serving as a major component in most of our modern industrial, transportations, medical, domestic, military, aerospace and other applications. One of the dominant factors of gears failure is the teeth fracture in the fillet region due to an intensive amount of tensile stress and stress concentrations, **(Robert**, **2013)**. Even though the early stresses analysis and Solution formulas for gears had been derived around the 19th century. However, these formulas are in most of the cases does not take into account the effect of the stress consecration factor. Moreover, although other investigators have considered this problem, their approaches for the determination of the necessary certain geometrical properties of the gear tooth shape such as tooth loading angle, tooth weakest section thickness, the load height from this section and Lewis form factor are usually graphical and approximated methods that simply represented the tooth fillet region by a straight line and a circular arc.

(Mitchinen, 1982). introduce a numerical technique in order to determine the tooth weakest section location, Lewis form factor (y) and AGMA geometry factor, based on the equations of the gear tooth profile that take into account the exact trochoid tooth fillet form developed by a generation process. His comparison results with Lewis (y) and AGMA (J) had proved to be much more accurate and the introduced technique is capable of evaluating (Y&J) of any gear teeth number of a standard spur gear tooth. **(Abdullah, 2012).** Presented an analytical method developed based on a previous trial graphical method, which was achieved to find the solution of bending stress equation for symmetric and asymmetric involute spur gear tooth. **(Moya, et al., 2010)** presented a theoretical analysis based on an iterative technique to determine Lewis form factor, which can play a major role in the fracture of asymmetric plastic gear teeth. **(Masuayma, et al., 2016).** conducted a 2D F.E simulation for investigating the bending strength of spur gears with symmetric, asymmetric fillets and asymmetric pressure angle and fillet teeth. It had been found that due to its great effect on tooth weakest section thickness the asymmetric unloaded side pressure angle value can help to reduce the amount of the induced bending stress, **(Hmoad et al., 2016. Hassan**, **2018).** formulated the required parametric equations for the generation or representation of the involute part and trochoid fillet part of spur gears. **(Kadum, et al., 2018).**

investigated the effect of using asymmetric higher value unloaded side pressure angle on bending stress in helical gears. Results shows that an asymmetric helical gear tooth with higher unloaded pressure angle can improve the gear bending strength. Moreover, a numerical Curve Fitted formula was formulate for the estimation of helical gear tooth stress concentration factor.
In this research, a developed analytical technique for the determination of tooth weakest section dimensions has been accomplished based on a prior numerical method (that had include standard involute profile only). It uses trochoid fillets that their equations have been extracted or derived based on a real gear generation method instead of the previous literature approximations that simply represented the tooth fillet region by a straight line and a circular arc. Which enables the determination of the location of the tooth weakest section based on the exact tooth profile. Hence an analytical solution for the Maximum tooth tensile stress and the combined fillet tensile stress concentration factor (Kst) for standard, asymmetric fillet radiuses, asymmetric pressure angle, and profile shifted (also known as non-standard or +eV and –eV profile shifted) involute helical and spur gears.

2. GEAR DIMENSIONS

All the dimensions of Standard and Asymmetric Spur gears can be calculated in terms of the gear teeth number, pressure angle and its module, **(Ugural, 2015)**. In addition, it should be noted that the generation and the working dimensions are the same for the standard gears. Which are:

$$R_{pj} = 0.5 * m_o * Zj \quad (1)$$
$$h_a = h_{af} * m_o \quad (2)$$
$$h_d = h_{df} * m_o \quad (3)$$
$$r_{fj} = R = rcj = r_{cfj} * m_o \quad (4)$$
$$R_{aj} = R_{pj} + h_a \quad (5)$$
$$R_{dj} = R_{pj} - h_d \quad (6)$$
$$R_{bj} = R_{pj} * \cos(\phi) \quad (7)$$

Positively or negatively shifted gears will have two sets of dimension, generation (constant) dimensions and working (variable) dimensions. Which are given below, (**Ugural, 2015)**:
Generation dimensions:

$$R_{Gj} = R_{pj} = 0.5 * m_o * Zj \quad (8)$$
$$h_{acj} = (h_{af} * m_o) + (xj * m_o) \quad (9)$$
$$h_{dcj} = (h_{df} * m_o) - (xj * m_o) \quad (10)$$
$$R_{acj} = R_{awj} = R_{pj} + h_{acj} \quad (11)$$
$$R_{dcj} = R_{dwj} = R_{pj} - h_{dcj} \quad (12)$$
$$R_{bcj} = R_{bwj} = R_{bj} = R_{pj} * \cos(\phi) \quad (13)$$
$$TH_{cj} = (0.5 * л * m_o) - (2 * xj * m_o * tan\,\phi) \quad (14)$$
$$TP_{cj} = (0.5 * л * m_o) + (2 * xj * m_o * tan\,\phi) \quad (15)$$
$$b_{cj} = h_{dc} - Rj \quad (16)$$
$$L_{cj} = \frac{TH_{cj}}{2} - b_c * \tan(\phi) - \frac{Rj}{\cos(\phi)} \quad (17)$$
$$w_{cj} = [0.5(TH_c + TP_c) - L_{cj}]/R_{Gj} \quad (18)$$

Working dimensions, Risitano, 2011:

$$[\tan\phi_w - \phi_w] = \frac{2(x_{l1}+x_{l2})\tan\phi}{Z_1+Z_2} + [\tan\phi - \phi] \quad (19)$$

$$R_{pwj} = R_{pj}\frac{\cos\phi}{\cos\phi_w} \quad (20)$$

$$R_{bwj} = R_{pwj}\cos\phi_w = R_{pj} * co\,s(\phi) = R_{bcj} = R_{bj} \quad (21)$$

$$h_{aw} = R_{awj} - R_{pwj} \quad (22)$$

$$h_{dw} = R_{pwj} - R_{dwj} \quad (23)$$

Helical gears in the transverse plane are similar to spur gear and the relations above for spur gears can be applied to helical gears. However, it should be noted that helical gears have the following relations that should be applied to spur dimensions, (**KHK Gears, 2015)**:

$$m_t = m_o/\cos(\beta_{\hbar}) \quad (24)$$

$$\phi_{ti} = \tan^{-1}(\frac{\tan(\phi_{ni})}{\cos(\beta\hbar)}) \quad (25)$$

$$x_{nij} = x_{tij}/\cos(\beta\hbar) \quad (26)$$

And $\phi_{ni} = \phi i$

3. ANALYTICAL SOLUTION OF MAXIMUM FILLET TENSILE STRESS and STRESS CONCENTRATION FACTOR

Before starting any analytical gear tooth stress analysis, it is necessary to identify certain geometric properties of the gear tooth profile shape including tooth-loading angle, the thickness of tooth weakest section and the height of the applied load from this section, which are essential to evaluate the tooth bending stress.

3.1. Determination of the Location of Tooth Weakest Section

The most - recognized formulations considering the problem of gear bending stress in the field of gear design are Lewis equation and AGMA equation (which based on the Lewis formula). However, the geometric factors that used in these two equations (Lewis form factor Y and AGMA geometry factor J) were determined graphically and in some instances are not sufficiently accurate nor convenient to use. Although other investigators have considered this problem, their methods are either very complicated analytically or graphical, (**Mitchinen, 1982).**

In this approach a numerical and developed analytical technique based on a prior numerical method by **(Mitchinen, 1982)** for standard involute profile has been developed to determine the location of tooth weakest section of standard, asymmetric trochoidal fillets, asymmetric pressure angle and Non-standard (+ve and –ve profile shifted gears) involute helical and spur gear modification technique.

We have reformulated the parametric equations for gear tooth trochoidal fillet region coordinate to take into account the standard, asymmetric trochoidal fillets, asymmetric pressure angle, and the non-standard gears in the global Cartesian coordinates with the Y-axis passing through the center of the tooth, as follow:

As shown in **Fig.1**, when the rack cutter shown in **Fig.2** translate by amount of (TP+TH), the working piece (generated gear) rotate by an amount of ($\frac{(TH+TP)}{R_G}$), this angle of rotation as illustrated in **Fig.3** is equal to:

$$\frac{(TH+TP)}{R_G} = 2(w+v) \quad (27)$$

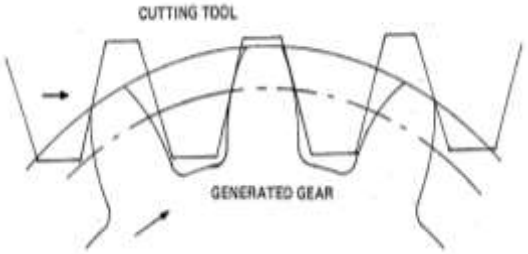

Figure 1. Generating a gear tooth, Lynwander, 1983.

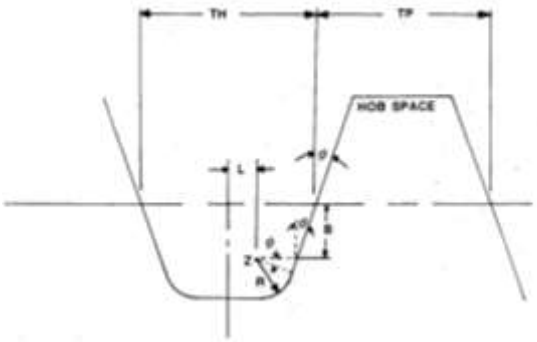

Figure 2. Hob or rack cutter geometry, Lynwander, 1983.

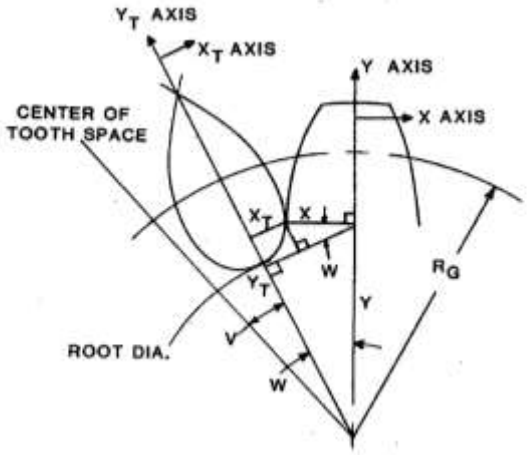

Figure 3. Root fillet trochoid and involute, Lynwander, 1983.

By referring to **Fig.2and Fig.3**, we can find the angles (v and w).

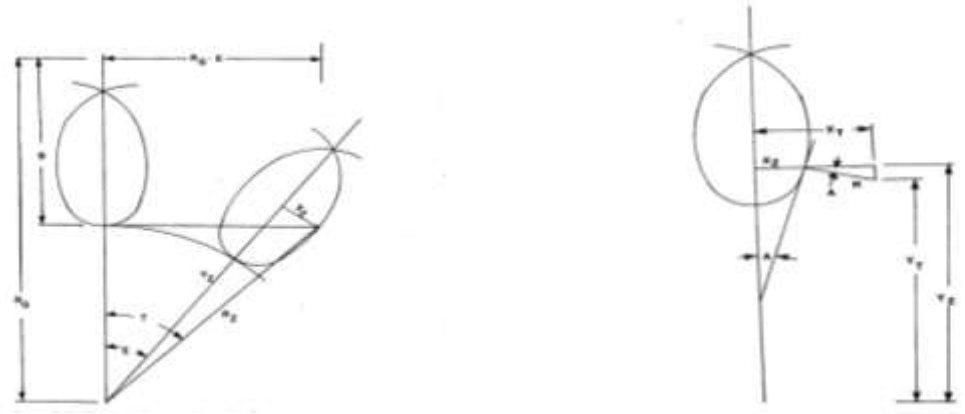

Figure 4. a) Trochoid generated by point Z, **b)** Trochoid coordinates in global X and Y system generated by the rounded corner of the rack tip, Lynwander, 1983.

Fig. **(4.a)** shows the trochoidal arc generated by the center point of the corner tip arc (point z). By applying coordinate transformation, the Cartesian coordinates of the trochoidal arc generated by the rounded corner of the rack tip in the global X and Y system can be found as illustrated in **Fig**. **4.** The final form of these parametric equations for gear tooth trochoidal fillet region are given by:

$$X = [[[(R_G * E)\, sinE + (R_G - b)\, cosE]] - Rsin(tan^{-1}[-(R_G * E)\, sin(E) + b * cos(E)]/[-R_G * sin(E) + b * sin(E) + [R_G * E * cos(E)] + R_G * sin(E)])] * \sin(w) - [[[(R_G * E)\, cosE - (R_G - b)\, sinE]] + Rcos(tan^{-1}[-(R_G * E)\, sin(E) + R_G cos(E) - R_G cos(E) + b * cos(E)]/[-R_G * sin(E) + b * sin(E) + [R_G * E * cos(E)] + R_G * sin(E)])] * cos(w) \quad (28.a)$$

$$Y = [[[(R_G * E)\, sinE + (R_G - b)\, cosE]] - Rsin(tan^{-1}[-(R_G * E)\, sin(E) + b * cos(E)]/[-R_G * sin(E) + b * sin(E) + [R_G * E * cos(E)] + R_G * sin(E)])] * cos(w) + [[[(R_G * E)\, cosE - (R_G - b)\, sinE]] + Rcos(tan^{-1}[-(R_G * E)\, sin(E) + R_G cos(E) - R_G cos(E) + b * cos(E)]/[-R_G * sin(E) + b * sin(E) + [R_G * E * cos(E)] + R_G * sin(E)])] * sin(w) \quad (28.b)$$

Where: E: a generation angle from (0 to 1) rad. Where in in the case of the location of tooth weakest section (point E' in **Fig**. 5) the angle (E) at point E' is equal to the root (χ).

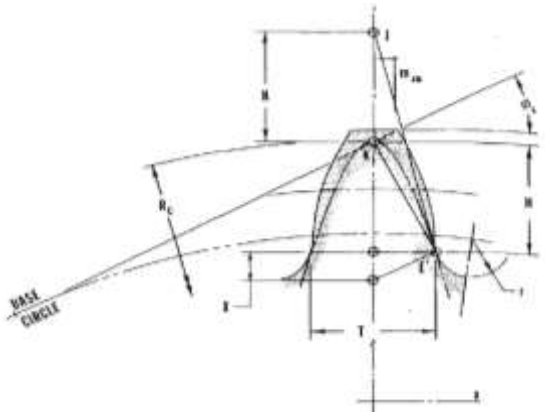

Figure 5. Tooth form factor geometry when the load acts at the tip of one tooth, Mitchiner, 1982.

In Wilfred Lewis approach the line of action intersects with the centerline of the gear tooth at the apex (point k) of the incised Parabola, that is tangent to the tooth root (fillet). The location of the tangency point and the slope of the tangent to the fillet are the main interest in the geometry factors computation.

In **Fig**.5, when the line of action passes out of the tooth tip. The slope of the tangent (line JE) can be given by (**Mitchinen, 1982):**

$$m_{JE} = -\frac{[1+\frac{b}{R_P}tan(w+\mathfrak{X})]}{[\frac{b}{R_P}-\tan(w+\mathfrak{X})]} \quad (29)$$

In addition, the intersection of that line with the centerline of the gear tooth at the apex of the parabola point is at a radius equals to:

$$Rc = [\frac{Rp*cos(\phi)}{cos\left(3-\left(\left(\frac{\pi}{2*Z}\right)+(tan(\phi)-(\phi))-(tan(3)-(3))\right)\right)}] \quad (30)$$

$$3 = \tan^{-1}[\frac{\sqrt{(1-((\frac{R_P}{R_a}*\cos(\phi))\hat{}2))}}{\frac{R_P}{R_a}*cos(\phi)}] \quad (31)$$

Sub Eq. (31) in Eq. (30) we get RC equals' to:

$$\boldsymbol{Rc} = [Rp*cos(\phi)\,]/COS\left([\tan^{-1}[\frac{\sqrt{(1-((\frac{R_P}{R_a}*\cos(\phi))\hat{}2))}}{\frac{R_P}{R_a}*cos(\phi)}]]-\left(\left(\frac{\pi}{2*Z}\right)+(tan(\phi)-(\phi))-\left(tan\left(\tan^{-1}[\frac{\sqrt{(1-((\frac{R_P}{R_a}*\cos(\phi))\hat{}2))}}{\frac{R_P}{R_a}*cos(\phi)}]\right)-\left(\tan^{-1}[\frac{\sqrt{(1-((\frac{R_P}{R_a}*\cos(\phi))\hat{}2))}}{\frac{R_P}{R_a}*cos(\phi)}]\right)\right)\right)\right) \quad (32)$$

The above-evaluated (Rc) in eq. (32) is for the determination of the geometry factors when the load acts at the tip of one tooth i.e. no load sharing for standard and non-standard gear. Noting that for non-standard gears the generation dimensions (not the working dimension) should be used instead of the standard dimensions to evaluate (Rc) and hence the root ($\mathfrak{X}$).

For the case of load sharing (or single tooth at HPSTC), as illustrated in **Fig. 6**. Then Rc can be derived from **Fig. 6** for standard and non-standard gear. Noting the for non-standard gears the working dimension should be used instead of the standard dimensions to evaluate (Rc_{sh}) while the generation dimensions should be used for the X and Y coordinates of the weakest point in equation (43) in order to find the root ($\mathfrak{X}$).

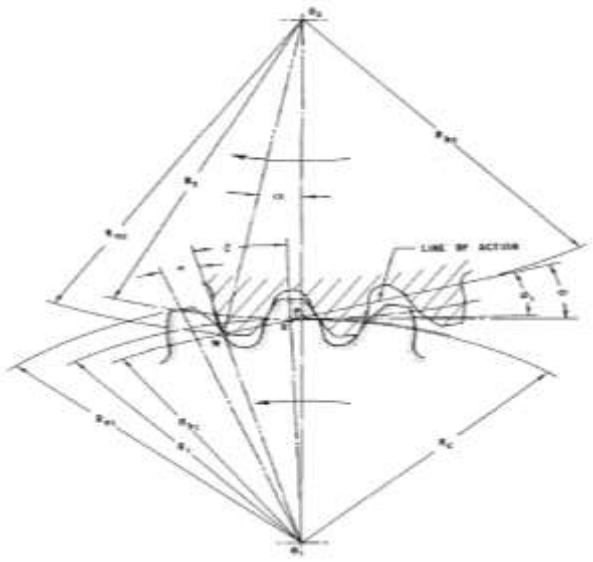

Figure 6. Tooth geometry when the load acts at HPSTC, Mitchiner, 1982.

Now from **Fig.** 6. (Rc) can be derive noting that:

$$Rc)_{sh} = (Rx * \sin(\zeta))/\sin(\zeta + \xi) \quad (33)$$

Where:

$$Rx = \sqrt{(Ð^2 + R_{p1}^2 - 2 * Ð * R_{P1} * \sin(\phi)} \quad (34)$$

Where:

$$Ð = R_{p2}\frac{\cos(ʂ+\phi)}{\sin(ʂ)} \quad (35)$$

$$ʂ = \sin^{-1}\{\frac{R_{p2}}{R_{a2}} * \cos(\phi)\} \quad (36)$$

Where:

$$\zeta = \cos^{-1}(\frac{R_x^2+R_{a2}^2-[R_{p1}+R_{p2}]^2}{2*R_x*R_{a2}}) - ʂ \quad (37)$$

$$\xi = \frac{2Л}{Z_1} - ƙ \quad (38)$$

Where

$$ƙ = \frac{Л}{2*Z1} - \left[\tan\left(\cos^{-1}\left(\frac{R_{p1}}{Rx} * \cos(\phi)\right)\right) - \left[\cos^{-1}\left(\frac{R_{p1}}{Rx} * \cos(\phi)\right)\right]\right] + [\tan(\phi) - \phi] \quad (39)$$

After we located point K, the next step in the determination of the geometry factors involves the specification of the Parabola. Which has its vertex at K and is tangent to the root (fillet). A parabola with its vertex at K and Pass into any point, such as E' will be tangent to a line JE'. Where the vertical distances between K and E' and J and K are equal, **(Mitchinen, 1982).** This is distance H in the **Fig. 5.** The above condition led to the following relations:

$$-\frac{(2*h)}{(0.5*t)} = m_{JE} \quad (40)$$

Moreover, since: $0.5t = X_E$ and $h = R_c - Y_E$ (41)

Those, Eq. (40) can be express as:

$$mje + \left(\frac{2*(R_c-Ye)}{Xe}\right) = 0 \quad (42)$$

Since Y_E, X_E, and m_{je} are function of Ƛ, Eq. 4.6 can be express as:

$$F(Ƛ) = mje(Ƛ) + \left(\frac{2*(R_c-Ye(Ƛ))}{Xe(Ƛ)}\right) = 0 \quad (43)$$

By the substitution of Equations (27), (28), (29) and {(32) or (33)} in equation (42), we get the expression of Eq. above in terms of the gear parameters and the root 𝔛. **The root (𝔛) can be evaluate by two methods:**

Method 1:

The first method is simpler than the second one in which an iterative technique based on Secant Method, Which considered as the most prevalent method of roots computation, (**Chapra, 2018).** have been used for this method to find the root 𝔛 of equation (43).

By applying the Secant method to equation (43) the formula of this method can be found by taking two initial guesses $\mathfrak{X}_{n-2}$ and $\mathfrak{X}_{n-1}$:

$$\mathfrak{X}_n = \mathfrak{X}_{n-1} - F(\mathfrak{X}_{n-1})\frac{(\mathfrak{X}_{n-1}-\mathfrak{X}_{n-2})}{F(\mathfrak{X}_{n-1})-F(\mathfrak{X}_{n-2})} \quad (44)$$

For fast convergence, the initial values are to be taken in the range of (0.2 rad to 0.05rad) for the small and large number of teeth respectively. The value of root 𝔛 usually achieves convergence to eight digits in just six iterations.

Method 2:

In this method, a direct analytical solution to evaluate the value of the root 𝔛 of equation (43) and hence, the geometry factors and the bending stress equation can be archived. Equation (43) is non-linear. In order to find the root of an angle 𝔛 an iterative technique based on the Newton-Raphson method **Chapra, 2018** have been used for this purpose. By applying the Newton-Raphson method to equation (43) the formula of this method can be found by taking an initial guess $\mathfrak{X}_n$:

$$\mathfrak{X}_{n+1} = \mathfrak{X}_n - \frac{F(\mathfrak{X}_n)}{f'(\mathfrak{X}_n)} \quad (45)$$

The Newton- Raphson algorithm is the best-known method of finding roots because it is simple and fast but this method is usable only in the problems where the derivative of the function can be readily computed.

The derivative of equation (43) in terms of gear constants, Rc and the angle root 𝔛 had been found equals to:

$$f'(\mathfrak{X}_n) = -2(\boldsymbol{RC} - Z8 - ZA - rf * Z6)(-Z3 * ZD - Z5^2 - 1) + (Z7 - Z3\,Z5\,ZD + Z5^2\,Z7)(-Z9 + ZB - rf(Z1\,ST\,Z7 + Z1\,CT)) + (Z8 + ZA - RP\,CT - rf(-Z1\,Z3\,ST\,ZD) - Z1\,ST + Z1\,CT\,Z7 + Z3^2\,CT\,ZC\,ZF + Z3^2\,ST\,ZC\,ZE))(Z5\,Z7 + 1) - 2(-Z5 + Z7)(-Z9 - RP\,ST - rf(Z1\,Z3\,CT\,ZD + Z1\,ST\,Z7 + Z1\,CT) + Z3^2\,ST\,ZC\,ZF) - Z3^2\,CT\,ZC\,ZE)) \quad (46)$$

Where:

$ZF = 1/((\mathfrak{X}\text{^}2) * (Rp\text{^}2))$, $ZD = 1/((\mathfrak{X}\text{^}2) * Rp)$, $ZC = b\text{^}2/(\mathfrak{X}\text{^}2 * Rp\text{^}2) + 1$

$ZB = (Rp - b) * sin(w + \mathfrak{X})$, $ZA = (Rp - b) * cos(w + \mathfrak{X})$, $Z9 = \mathfrak{X} * Rp * cos(w + \mathfrak{X})$

$Z8 = \mathfrak{X} * Rp * sin(w + \mathfrak{X})$, $Z7 = b/(\mathfrak{X} * Rp)$, $Z5 = tan(w + \mathfrak{X})$

$Z6 = b * (-b * cos(w + \mathfrak{X}))/(\mathfrak{X} * Rp) + sin(w + \mathfrak{X}))/(\mathfrak{X} * Rp)$, $CT = cos(w + \mathfrak{X})$

$ST = sin(w + \mathfrak{X}), Z4 = 1/(\mathfrak{X} * Rp)$, $Z3 = b$, $Z2 = Rp - b$, $Z1 = b/(\mathfrak{X} * Rp)$

The main advantage of this technique its rapid convergence to the final root. Often three iterations are sufficient. Also, it can be reduced these iterations by using a closer starting guess of the root (𝔛) and from the previous knowledge of involute tooth profile construction the working range of angle (𝔛) may be about (Л/16 to Л/64) for small number and large number of

teeth gear respectively). Therefore, with some mathematical configurations it can be found a direct solution rather than an iterative solution, as shown below:
By applying Equation (43) and (46) in equation (45) with initial value of (Л/24), it can be find that:

$$\text{Xo} = \frac{Л}{24} \quad (47)$$

$$\text{X1} = \text{Xo} - \frac{F(\text{X}_o)}{f'(\text{X}_o)} \quad (48)$$

$$\text{X2} = \text{X1} - \frac{F(\text{X}_1)}{f'(\text{X}_1)} \quad (49)$$

The expression of (X2) in equation (49) represents the final expression of (X), with the error tolerance, ε= X2 − X1 < $1 * 10^{-4}$. Once the angle root (X) has been found the point of the tooth root (fillet) weakest section by applying equation (27) and (28). Then by applying equation (41), the tooth weakest section thickness (t) and the height of load from the weakest section (h) can be determined.

3.2 Calculations of Lewis Form Factor

In 1892, Wilfred Lewis announced his famous equation, which still the basis for most gear design today **(Ugural, 2015)** to evaluate the value bending stress at tooth root fillet of **spur and helical** gears. Where (**Budynas, et al., 2010):**

$$\sigma_b = \frac{Ft}{w_Ж * m_o * Y} \quad (50)$$

$$Y = \frac{2\text{X}}{3m_o} = \frac{t^2}{6 * m_o * h} \quad (51)$$

Where Y is the Lewis form factor of standard gears only and it obtained from standard tables **(Budynas, et al., 2010).** Where this factor considers only the effects of bending on the tooth element, not the combined effects of bending and compression.
In this research, an alternative technique to evaluate the (Y) for standard, symmetric and profile shifted {also known as Non-standard or (+eV and –eV profile shifted gears)} gear tooth has been carried out by substituting (t) and (h) from the developed analytical equations of equation (49) by equation (41) in equation (51). In addition for the case of asymmetric fillets tooth and asymmetric pressure angle gears by the assuming that the tooth centerline remains the same for the two sides of the gear tooth, the same technique is used but by replacing the tooth thinness (t) in equation (51) by ($t' = 0.5t_l + 0.5t_u$) and letting $h = h_l$.

3.3 Determination of the Gear Tooth Maximum Tensile Stress and Stress Concentration Factor

The most well-known formulation addressing the problem of gear stress concentration factor that is considered as the most reliable equations and had been adopted by the American Gear Manufacturers Association for the calculation of combined tensile stress concentration factor is the formulas of Combined tensile stress concentration factor (Kst) introduced by Dolan and Broghamer **(Budynas, et al., 2010).** Which are empirical equations based on extensive photoelastic research regarding the mater of this factor given by **(Budynas, et al., 2010):**

$$k_{st} = Ч + \left[\left[\frac{t}{Я}\right]^{ъS} * \left[\frac{t}{h}\right]^{ыS}\right] \quad (52)$$

Where:

$$Ч = 0.34 - [0.4583662 * \phi] \quad (53)$$

$$ъS = 0.316 - [0.4583662 * \phi] \quad (54)$$

$$ыs = 0.290 + [0.4583662 * \phi] \quad (55)$$

$Я = r_f + ((b^2)/(R_p + b))$ (56)

However, the main problem of this approach is that it requires geometry factors (t and h) that depends on graphical techniques such as of AGMA and Dolan and Broghamer and in some instances these graphical techniques are not convenient to use nor sufficiently accurate. Although other investigators have considered this problem, their methods are either graphical or very complicated analytically Mitchiner, 1982.

In this research, an alternative technique to evaluate the (Kst) analytically has been carried out by substituting (t) and (h) from the direct analytical equations of equation. (49) by equation (41) in equation (52). Therefore, after we have evaluated the value of (Kst) then the maximum tensile stress at gear tooth fillet is equals to the flexural stresses minus the direct stress developed by the radial component then multiple by (Kst).

Therefore:

$\sigma_t = [\sigma_b - \sigma_c]$ (57) $\sigma_{t\,max} = [\sigma_b - \sigma_c] * k_{st}$ (58)

Sub. Eq. (50) in eq. (57) and eq. (58) we get then the nominal tooth tensile stress and maximum tooth tensile stress, which is, equals to:

$\sigma_t = \left[\left[\frac{Ft}{w_f * m_o * Y}\right] - \left[\frac{Fr}{(t * w_f)}\right]\right]$ (59) $\sigma_{t\,max} = \left[\left[\frac{Ft}{w_f * m_o * Y}\right] - \left[\frac{Fr}{(t * w_f)}\right]\right] * k_{st}$ (60)

The Combined tensile stress concentration factor (Kst) and the maximum tooth tensile stress for symmetric, profile shifted {also known as Non-standard or (+eV and –eV profile shifted gears)}, asymmetric fillets and asymmetric pressure angle gear tooth can be evaluated by applying the same techniques that have been mentioned before above in the evaluating of non-standard Lewis form factor.

Definition of the stress concentration factor by

(Paul, 2010). as the ratio of the maximum numerical stress magnitude by the analytical nominal stress magnitude. Therefore another equation to evaluate the value of (Kst), which has been used to verify the results of (Kst) of eq. (52) and hence the values of maximum tooth tensile stress computed analytically by equation (60), is given by

$k_{st}{}' = \frac{\sigma_{t\,max})_{by\ FEM}}{\sigma_t}$ (61)

Equation (44) of the numerical iterative first method and equation (49) of the second direct solution method with the other related equations have been programmed in FORTRAN language. With the gear parameters and the initial guesses as input data and the value of the root (Ɤ), Lewis(Y) form factor, stress concertation (k_{st}) factor, the nominal bending stress, nominal tensile stress and the maximum tooth tensile fillet stress as output data for symmetric, Profile shifted, asymmetric fillets and asymmetric pressure angle involute helical and spur gears (with a number of teeth equals to the virtual number of teeth (Zv) gears.

3.4 Derivation of the Tooth Loading Angle of Standard and Non-Standard (+ve & -ve Profile Shifted) Spur and Helical Gears

In order to design and analyze a variety of standard and Non-Standard gear tooth profiles by analytical or numerical analysis the tangential(F_t) (horizontal), radial(F_r) (vertical) force components and even the axial force component (F_{axi}) in the case of helical gears of the normal applied force are required. Especially, when the analyzation is in the case of extreme and worst

loading condition (load acting at the gear tip i.e. R2=Ra). **Fig.** 7and **Fig.8** Illustrates the normal force components of spur and helical gears respectively.

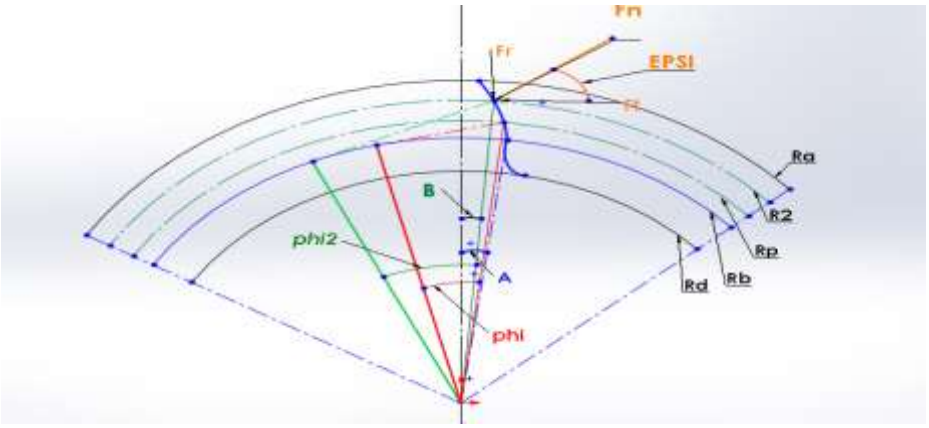

Figure 7. Components of tooth normal force in a spur gear.

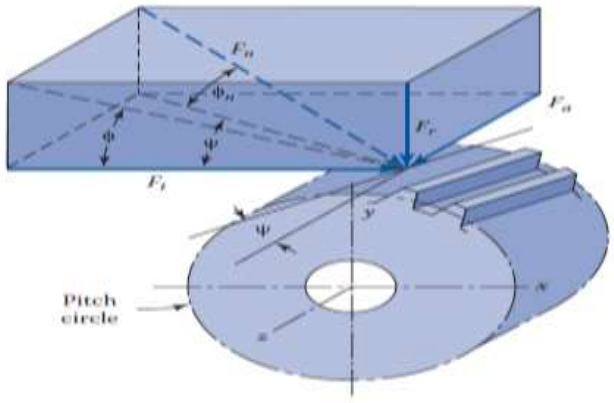

Figure 8. Components of tooth normal force in a helical gear, **Ugural, 2015.**

A normal force (F_n) can act at any location on the active involute profile portion of the loaded side. From **Fig. 7**, with (F_n) act at a radius *R2* from the gear center. We could see that:

$\Psi = \phi 2 - \text{В}$ (62)

In **Fig. 4** at the generation radius, (pitch radius):

$R_1 = R_G = R_p$ (63)

$\Phi_1 = \phi$ (64)

$\Theta_1 = [\tan(\Phi_1) - \Phi_1 \ ]$ (65)

$CCT_1 = TP$ (66)

$For\ standared\ gears\ TP = TH = 0.5 * \text{л} * m_o$ (67)

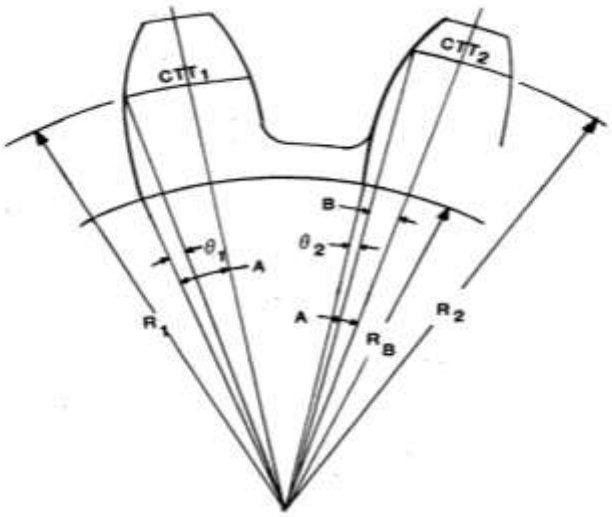

Figure 9. Tooth thickness calculation, Lynwander, 1983.

Referring to **Fig. 9**, the angle (A) can be found by:

$$A = \Theta_1 + (0.5 * CCT_1)/ R_1 \quad (68)$$

When the circular tooth thickness (CCT_1) at the generating pitch R_G radius known the thickness at any other radius R_2 (where $R_B \leq R2 \leq R_a$) can be calculated from **Fig.** 9 by:

$$\Theta_2 = \tan(\phi_2) - \phi_2 \quad (69)$$

$$\phi_2 = \cos^{-1}(\frac{R_b}{R_2}) \quad (70)$$

Thus, the circular thickness at R_2 is equal to:

$$CCT_2 = 2 * R_2 * [\left(\frac{0.5*CCT_1}{2}\right) + \Theta_2 - \Theta_1] \quad (71)$$

$$angle\ B = \frac{0.5*CCT_2}{R_2} = A - \Theta_2 \quad (72)$$

By substituting equation (64) in (65) then with eq. (63) in eq.(68) and with eq.(70) in eq.(69) and substituting the resulted equations in equation (71) and finally in equation(72) we get the value of the angle B, which equals to :

$$\mathcal{B} = \{[\tan(\phi) - \phi] + [(0.5 * TP)/ R_P] - [tan\left(cos^{-1}(\frac{R_b}{R_2})\right) - cos^{-1}\left(\frac{R_b}{R_2}\right)]\} \quad (73)$$

By substitute eq. (69) &. (73) in equation (62), we could found that:

$$\Psi = cos^{-1}(\frac{R_b}{R_2}) - \{[\tan(\phi) - \phi] + [(0.5 * TP)/ R_P] - [tan\left(cos^{-1}(\frac{R_b}{R_2})\right) - cos^{-1}\left(\frac{R_b}{R_2}\right)]\}$$

$$\therefore \boldsymbol{\Psi_{ij} = -\{[tan(\phi i) - \phi i] + [(0.5 * TP_{ij})/ R_{Pj}] - tan\left(cos^{-1}(\frac{R_{bj}}{R_2})\right)\}} \quad (74)$$

Therefore:

1. In case of standared and assymitric spur gears

$$\therefore \Psi_{ij} = -\{[tan(\phi i) - \phi i] + [(0.25 * л * m_o)/ R_{Pij}] - tan\left(cos^{-1}(\frac{R_{bj}}{R_2})\right)\} \quad (75)$$

2. In case of Non-standard {symmetric or asymmetric [pressure angles and (or) shift factors]} spur Gers:

$$\Psi_{ij} = -\{[tan(\phi i) - \phi i] + [\frac{[(0.25*л*m_o)+(xij*m_o*tan\phi)]}{R_{Pij}}] - tan\left(cos^{-1}(\frac{R_{bj}}{R_2})\right)\} \quad (76)$$

Where:

$$Ft = Fn * \text{Cos}(\Psi) \quad (77)$$

$$Fr = Fn * \text{Sin}(\Psi) \quad (78)$$

3. In Case of Standard and Non-Standard {Symmetric Or Asymmetric [Pressure Angles and (Or) Shift Factors]} Helical Gears:

$$\Psi_{ijt} = -\{[tan(\phi it) - \phi it] + [(0.5 * TP_{Ct)ij}/ R_{Pj}] - tan\left(cos^{-1}(\frac{R_{bj}}{R_2})\right)\} \quad (79)$$

$$\boldsymbol{\Psi_{ijn} = \tan^{-1}[\tan(\Psi_{ijt}) * \cos(\beta ħ)]} \quad (80)$$

Where:

$$Fr = Fn * \text{Sin}(\Psi n) \quad (81)$$

$$Ft = Fn * \text{Cos}(\Psi n) * Cos\ (\beta ħ) \quad (82)$$

$$F_{axial} = Fn * \text{Cos}(\Psi n) * Sin\ (\beta ħ) \quad (83)$$

4. Numerical (FE) Solution

In this part, The FE results of the gear tooth maximum tensile stress for different Gear samples of spur and helical gears by applying a 3D loading which acts at the gear tooth tip (i.e. no load sharing or unity contact ratio) in order to investigate the accuracy of the maximum tooth tensile stress analytical results and the stress concentration factor (K_{st}) evaluated by equation (60) and (52) respectively.

A computer -aided design software (SolidWorks Version 2017) has been programmed in order to generate accurate complete 3D models for the standard and non-standard helical and spur gears and provides the required digital files extension for the CAE software. The number and type of elements have been chosen according to the fastest and the most accurate converged results. A tetrahedral element type of initial size of (1 mm) has been used to generate a 3D mesh, which has been refined in the tooth fillet areas were the maximum stresses expected to be. The size of the elements in the tooth root (fillet) area is about (0.5mm to 0.01 mm). The elements number and size are not constant and it differs according to each gear type model according to the convergence test. However, the average numbers of elements and nodes are about (800,000) and (1,009,073) respectively. In the FE investigations for spur gears, the tangential (F_t) and the radial (F_R) force components of a normal force of magnitude (Fn =2400 N) acts on the gear tooth tip and inclined by a loading angle (Ψ_{ij}) have been applied (same loading condition of the analytical analysis). In Case of helical gears a 3D loading represented by the tangential (F_t), radial (F_R) and the axial (end thrust force (F_{axi})) force components of a normal force of magnitude (Fn =2400 N) acts on the gear tooth tip and inclined by a loading angle (Ψ_{ij}) have been applied. **Fig. 10 to Fig.15** shows the tooth maximum tensile stress distribution inside a gear tooth fillet for variety of spar and helical gear samples of different design parameters and non-standard modifications, their dimension given in **Table 4.** Investigation and comparison results are shown in **Tables 3** and **4.** The comparison results show an excellent agreement between the analytical and F.E results.

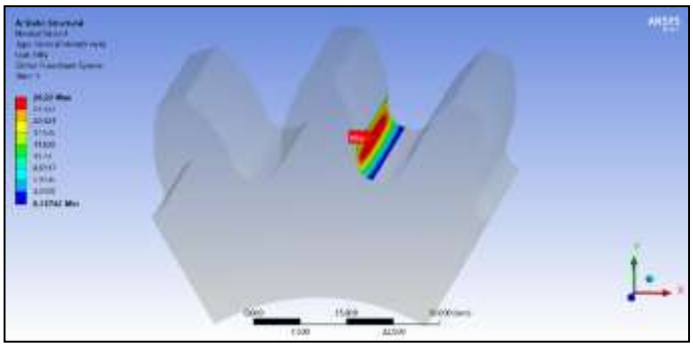

Figure 10. Gear Tooth Maximum Fillet Tensile Stress and Stress distributions of Standard Full depth, Gear Sample No.1

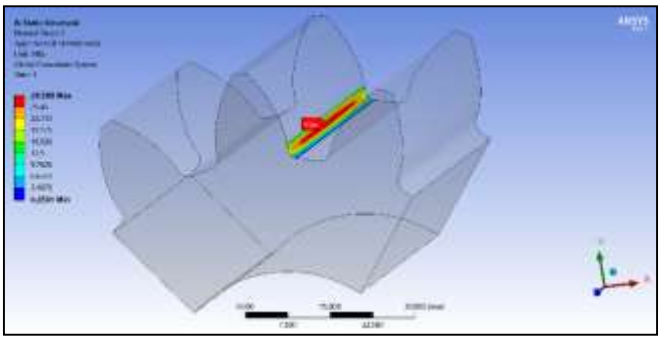

Figure 11. Gear Tooth Maximum Fillet Tensile Stress and Stress distributions of Non-Standard Spur gear, Gear Sample No.2.

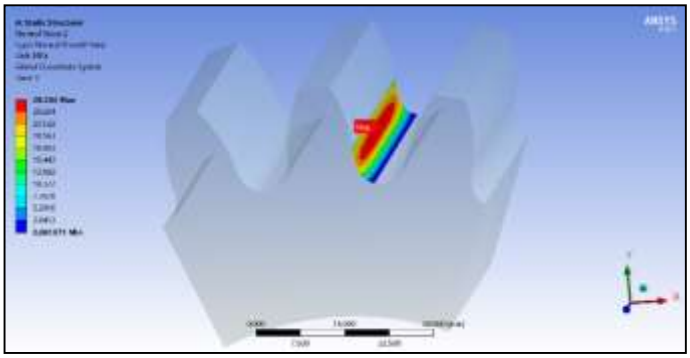

Figure 12. Gear Tooth Maximum Fillet Tensile Stress and Stress distributions of Non-Standard Spur gear, Gear Sample No.3.

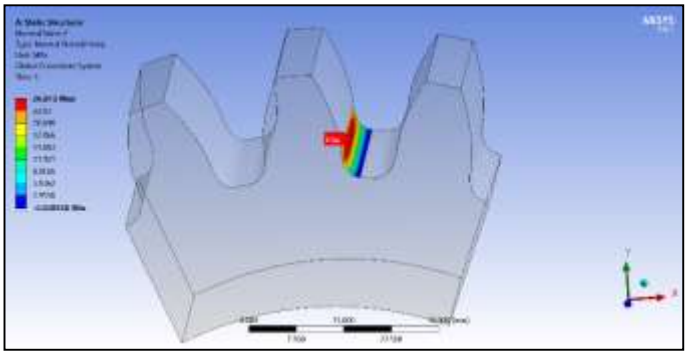

Figure .13 Gear Tooth Maximum Fillet Tensile Stress and Stress distributions of Asymmetric Spur gear, Gear Sample No.4

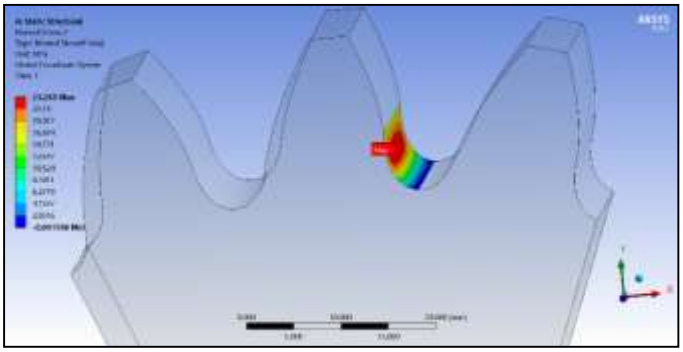

Figure 14. Gear Tooth Maximum Fillet Tensile Stress and Stress distributions of a Non-Standard {Negative Profile Shifted Asymmetric Gear} Spur gear, Gear Sample No.5.

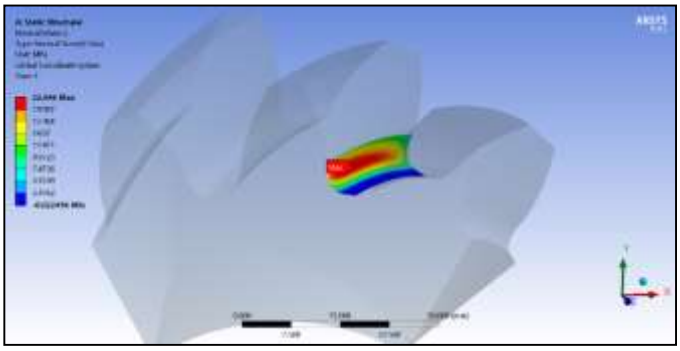

Figure 15. Gear Tooth Maximum Fillet Tensile Stress and Stress distributions of Standard Full depth Helical gear, Gear Sample No.6.

4. VERIFICATION OF THE DEVELOPED ANALYTICAL METHOD RESULTS

In order to verify the results of this research developed analytical method, three procedures have been used for this purpose. The first one is by comparing the results of Lewis form factor (Y) evaluated by this method with those of **Mitchinen, 1982**. Results are shown in **Tables 1 and 2.** The second procedure by comparing the value of the stress concentration (k_{st}) factor calculated analytically by equation (52) based on this method with the result of those of ($k_{st}{}'$)evaluated by equation (61) based on the nominal tensile fillet stress and the FE results. Results are shown in Table (6.3). In the third procedure, the calculated results of the maximum tensile fillet stress of spur and helical gears have been compared with results extracted from the FEM solution. Results are shown in **Fig. 10 to Fig.15** and **Table 4.** From the comparison results in **Table 1 to 4** it is clear that the developed analytical method of this research is very accurate in evaluating the value of the gear tooth maximum tensile stress, nominal tensile stress, nominal bending stress, combined stress concertation factor (K_{st}) and Lewis (Y) form factor for standard, symmetric, asymmetric fillets, asymmetric pressure angle and non-stranded (Profile Shifted) helical and spur gears analytically. From these comparisons, have been proven the validity of this research analytical and numerical results.

Table 1. Comparisons of Lewis form factor values evaluated by this research developed analytical method for Standard ($20^{0)}$ full depth involute spur gear teeth with the Standard published tables.

Number of Teeth	Z=12	Z=24	Z=100
Developed Analytical Method	0.2296009	0.3305571	0.4357427
Standard Lewis form factor *	0.2296	0.33056	0.43574
Discrepancy Percentage%	0.00039%	0.00087%	0.00061%

Table 2. Comparisons of Lewis form factor values evaluated by this research developed analytical method for Standard ($20^{0)}$ full depth involute Helical gear teeth with the Standard ones.

Number of Teeth	Z=15	Z=39
Helix angle	Bh=22.5^{o}	Bh=30^{o}
Developed Analytical Method**	0.3009353	0.4105186
Standard Lewis form factor ***	0.30078	0.41047
Discrepancy Percentage%	0.05%	0.01%

Where:

***** The value of Lewis form factor (*Y*) obtained from standard table, **(Mitchinen, 1982).**

** The value of Lewis form factor (*Y*) for helical gears obtained from eq.(51) at the virtual number of teeth.

** *The value of Lewis form factor (*Y*) for helical gears obtained from the standard table of **(Mitchinen, 1982).** at the equivalent (virtual) number of teeth which is equals to $\boldsymbol{Ze = \frac{Z}{COS^3(\beta h)}}$ for any helix angle.

Table 3. Comparisons of the stress concentration (k_{st}) value calculated analytically with those of (k_{st}') that based on the FE results.

Spur Gear*	
Helix angle	βh=0°
k_{st}	1.53
$t_{Total\ (mm)}$	13.275447
h	11.449860
Y	0.3664800
Ψ_L	25.60356°
Nominal fillet **Tensile** Stress (Mpa)	15.311
k_{st}'	1.52
Discrepancy Percentage%	**0.66 %**

Helical Gear**	
Helix angle	βh=22.5°
k_{st}	1.49
$t_{Total\ (mm)}$	12.998970
h	12.397130
Y	0.3245243
Ψ_{nL}	28.43305°
Nominal Fillet **Tensile** Stress (Mpa)	15.204
k_{st}'	1.48
Discrepancy Percentage%	**0.68%**

*****Non-Standard (Negative profile sifted asymmetric pressure angle) Spur gear when load acts at the tip of one tooth. [ΦL=20, Φu=30, XL=Xu= -0.3m_o, Z=24, rf= 0.3m_o, hd=1.25m_o, ha=1m_o, m_o=7], FEM-Solution in **Fig. 14.**

******Standard Full Depth 20°, Z=18, m_o=7 Helical gear when load acts at the tip of one tooth, FEM-Solution in **Fig. 15.**

Table 4. Comparisons of the maximum gear tooth fillet tensile stress values evaluated by this research developed analytical method for different gear types or gear samples with those of FE results.

Gear Sample No.	1	2	3	4	5	6
ΦL / Φu	20°/20°	14.5°/14.5°	20°/20°	20°/14.5°	20°/30°	20°/20°
ha	1m_o	1m_o	1m_o	1m_o	1m_o	1m_o
hd	1.25m_o	1.25m_o	1.25m_o	1.25m_o	1.25m_o	1.25m_o
rc	0.3m_o	0.209m_o	0.3m_o	0.3m_o	0.3m_o	0.3m_o
Z	18	14	24	24	24	18
mo	7	7	7	7	7	7
X	--	+0.5625m_o	-0.3m_o	--	-0.3m_o	--
βh	--	--	--	--	--	22.5°
t Total (mm)	12.34313	13.144730	11.71156	12.37543	13.275447	12.99897
h (mm)	12.36891	14.25673	11.44986	12.40532	11.44980	12.39713
Y	0.293271	0.2885586	0.285219	0.293943	0.366480	0.324524
$\sigma t\ max$) **Analytic (Mpa)**	26.31	28.838	28.556	27.225	23.475	22.9
$\sigma t\ max$) **FE (Mpa)**	26.22	28.588	28.244	26.813	23.263	22.466
Discrepancy Percentage	**0.34%**	**0.87**	**1.1%**	**1.5%**	**0.91%**	**1.93%**

1. Analytical investigations:

In this part, the effects of many design parameters on the values of gear tooth stress concentration factor have been investigated. We have been investigated the effects of the gear tooth pressure angle (Φ), profile shift factor (X_{ij}), number of teeth, gear module, the cutter tip radius factors or tooth fillet factors and fillets factors asymmetry, the helix angle (βḥ) and the unloaded side pressure angle on the values of gear tooth stress concentration factor.

2. Result and Discussion

The results date have been represented through different figures type (**Fig. 16 to Fig. 23**) to provide a clearer image on the effects of these parameters and modifications on the amount of the stress consternation factor (K_{st}).

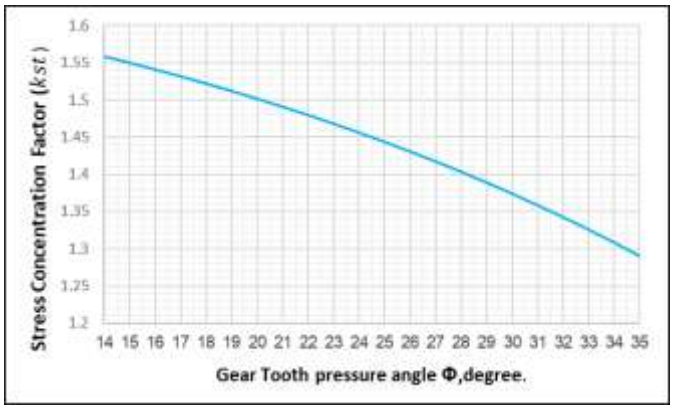

Figure 16. The effect of gear tooth pressure angle on the value of the Stress Concentration Factor (Kst).

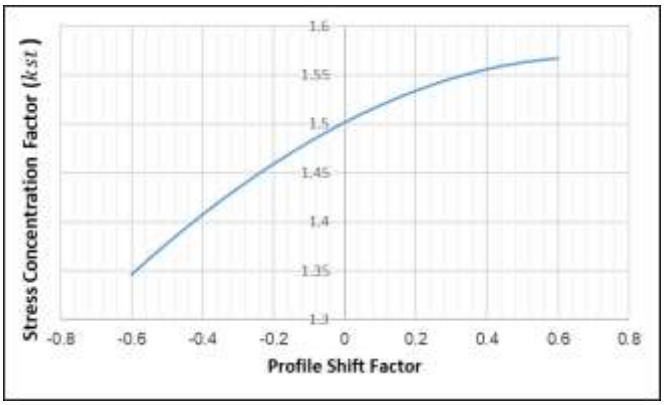

Figure 17. The effect of the profile shift factor on the value of the Stress Concentration Factor (Kst).

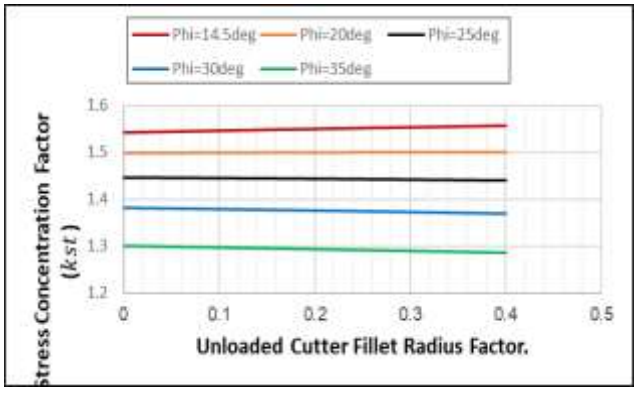

Figure 18. The effect of the Unloaded Side Cutter Fillet Radius Factor on the value of the Stress Concentration Factor (Kst), When rc loaded = 0.3mo.

Figure 19. The effect of the gear module on the value of the Stress Concentration Factor (Kst).

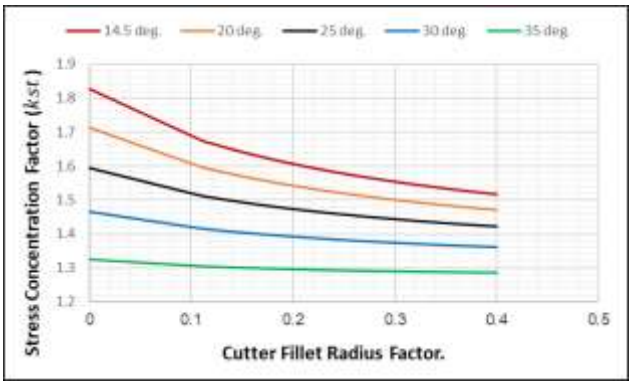

Figure 20. The effect of the Cutter Fillet Radius Factor on the value of the Stress Concentration Factor (Kst).

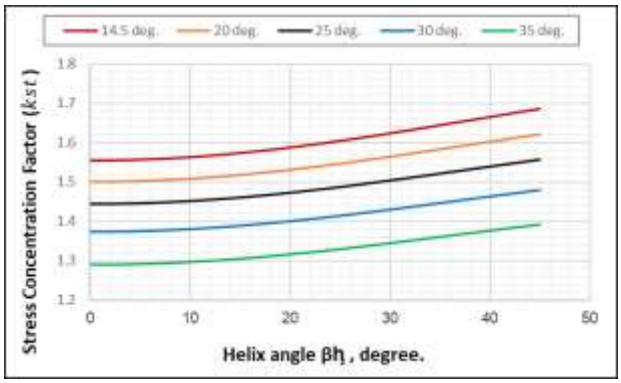

Figure 21. The effect of the helix angle on the value of the Stress Concentration Factor (Kst).

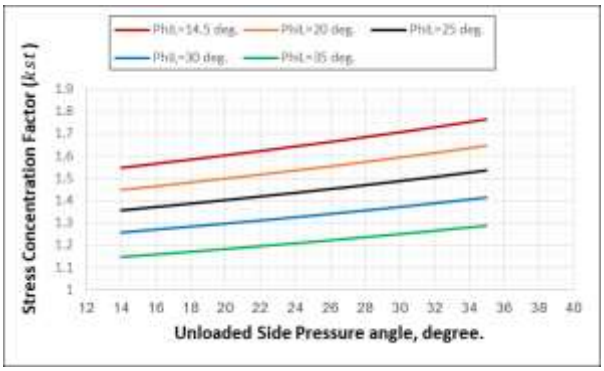

Figure 22. The effect of the Unloaded Side Pressure angle on the value of the Stress Concentration Factor (Kst).

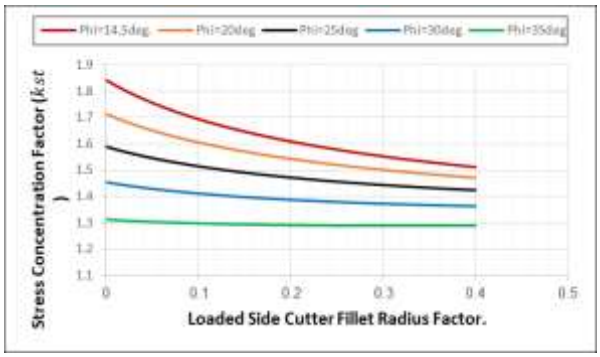

Figure 23. The effect of the Loaded Side Cutter Fillet Radius Factor on the value of the Stress Concentration Factor (Kst), When rc unloaded = 0.3mo

From these figures, we can summaries the investigation results in the following points:

1- Using a higher tooth pressure angle will greatly reduce the amount of the stress concentration factor. Which mean less maximum tensile stress and higher load carrying capacity.

2- Using a negative profile shifting modification technique will considerably decrease the amount of the stress constrain factor (***K**st*) leading to a higher load carrying capacity.

3- Using a positive profile shifting (or profile correction) will increase the amount of the stress concentration factor leading to higher maximum stresses, which decrease the gear tooth load carrying capacity.

4- Increasing the teeth number will increase the amount of the stress concentration factor to a certain value then the effect will become less and less sensible as teeth number increase.

5- Increasing or decreasing the gear module have no effects on the amount of the stress concentration factor (***K**st*). This is because the tooth will maintain its fixed shape and dimensions ratio for any gear module value.

6- Increasing the amounts of the cutter tip radius or tooth fillet radius generally greatly reduce the amount of the stresses concentration factor. However, this effect becomes much less sensible or effective as the gear tooth pressure angle increase. Therefore, we conclude that, for the lower

values of pressure angles (14.5, 20) degree, it is advisable to increase the fillet radius factor. However, the higher value of pressure angles (30, 35) degree can be design without a big attention to the value of tooth fillet radius, since it has no sensible or effective results.

7- The amount of stress concentration factor will increase by a slight amount after the gear tooth helix angle increases beyond a certain amount.

8- Using a higher loaded tooth side pressure angle with a lower value unloaded tooth side pressure angle will greatly reduce the amount of the stress concentration factor. Moreover, if a negative profile shifting applied on this asymmetric gear it can farther decrees the amount of stress concentration factor , which mean less maximum tensile stress and higher load carrying capacity

9- The loaded side root fillet radius has a dominant factor in compared with the unloaded side fillet radius in reducing the amount of induced stress concentration factor.

CONCLUSIONS

1- This research developed analytical method has been proved to be very accurate in determining the amount of nominal and maximum tensile stress and the stress concentration factor for standard and any other combination of non-standard modifications for involute helical and spur gears.

2- The most effective method for reducing the amount of induced stress concentration factor have been found by using asymmetric gear tooth with lower unloaded pressure angle side and with high loaded side pressure angle and fillet radius.

NOMENCLATURES

Symbol	Description	Units
CCT	circular tooth thickness	mm
Fn	Applied normal load	N
h	Load height from the tooth weakest section	mm
ha & hd	Tooth addendum and dedendum heights respectively	mm
Kst	Tooth combined tensile stress concentration factor	------
m_o	Module of gear	mm
m_{JE}	slope of line JE tangent to root fillet	------
rc	Fillet radius on rack-cutter tip	mm
t	Tooth weakest section thickness	mm
Ra	Radius of addendum circle	mm
Rb	Radius of base circle	mm
Rd	Radius of dedendum circle	mm
Rp	Radius of pitch circle	mm
TP,TH	circular tooth and space thickness respectively	mm
X	Profile Shift factor	------
Z	Number of teeth	------
Φ	Pressure angle	degree
Φw	Working pressure angle	degree
Ψ	Tooth loading angle	degree
βh	Helix angle	degree
ʂ, ζ , ƙ	Construction angles	degree

Ω	Angle between line of action and horizontal line	degree
θ	Involute function	rad

REFERNCES

- Abdullah, M, Q, 2012, *Enhancement of Gear Drive Performance Using an Alternative Design Approach of Teeth Profile* Doctorate dissertation, University of Baghdad, Collage of Engineering, Iraq.
- Budynas, R,G, and Nisbett, J, K,2015, Shigley's Mechanical Engineering Design, Tenth Edition, by McGraw-Hill Education, two Penn Plaza, New York.
- Chapra, S, C, 2018, Applied Numerical Methods with MATLAB for Engineers and Scientists", by McGraw-Hill Inc., New York, USA.
- Hassan, A, R, 2018, Pressure Angle and Profile Shift Factor Effects on the Natural Frequency of Spur Gear Tooth Design, World Academy of Science, Engineering and Technology International Journal of Mechanical and Mechatronics Engineering Vol: 12, No: 1.
- Hmoad, N, R. and Abdullah, M, Q, 2016, Analytical and Numerical Tooth Contact Analysis (TCA) of Standard and Modified Involute Profile Spur Gear, Journal of Engineering, Number 3 Volume 22.
- Kadum, A, M, and Abdullah, M, Q, 2018, "Stress Concentration factor Analysis of Helical Gear Drives with Asymmetric Teeth Profiles, Journal of Engineering, No.5 Volume 24.
- KHK Gears, 2015, CALCULATION OF GEAR DIMENSIONS, Kohara Gear Industry Co, Japan.
- Lynwander, P, 1983, "GEAR DRIVE SYSTEMS DESIGN AND APPLICATI" by MARCELDEKKER, INC. New York and Basel.
- Masuyama, T, MIMURA, Y, and Inoue K, 2016, bending strength simulation of asymmetric involute tooth gears, Bulletin of the JSME Journal of Advanced Mechanical Design, Systems, and Manufacturing, Vol.9, No.5, Japan.
- Mitchiner, R, G, and Mabie, H, H, 1982, The Determination of the Lewis Form Factor and the AGMA Geometry Factor J for External Spur Gear Teeth, ASME paper,Vol. 104, January.
- Moya, J, L, Machado, A, S, Velasquez, J. A., Goytisolo, R., Hernandez, A. E., Fernandez, J. E., and Sierra, J. M., 2010, A Study in Asymmetric Plastic Spur Gears, Gear Solutions, USA, April, pp.32-41.
- Paul , I, D,2010, Modification of Spur Gear Using Computation Method-Involutes Profile Being Modify, International Conference on Industrial Engineering and Operations Management Dhaka, Bangladesh, Januar.
- Risitano, A, 2011, Mechanical Design, by Taylor and Francis Group, LLC.
- Robert, L, N, 2013, Machine Design an integrated approach, fifth Edition, by Pearson prentice Hall Inc.
- Ugural, A, C, 2015, MECHANICAL DESIGN OF MACHINE COMPONENTS, SECOND EDITION, by Taylor & Francis, L Boca Raton London New York.